Supplemental Material

Journal of Climate
Linking Projected Changes in Seasonal Climate Predictability and ENSO Amplitude
https://doi.org/10.1175/JCLI-D-23-0648.1

Supplementary Material for:

Linking projected changes in seasonal climate predictability and ENSO amplitude

Dillon J. Amaya[1], Nicola Maher, Clara Deser, Michael G. Jacox[1,2], Matthew Newman, Michael A. Alexander[1], Juliana Dias, and Jiale Lou

[1]Physical Science Laboratory, Earth System Research Laboratory, National Oceanic and Atmospheric Administration, 325 Broadway, Boulder, CO 80305, United States
[2]Environmental Research Division, Southwest Fisheries Science Center, National Oceanic and Atmospheric Administration, 99 Pacific St #255A, Monterey, CA 93940, United States
[3]Cooperative Institute for Research in Environmental Sciences, University of Colorado Boulder, 216 UCB, University of Colorado Boulder campus, Boulder, CO 80309, United States
[4]National Center for Atmospheric Research, 1850 Table Mesa Dr, Boulder, CO 80305, United States

Corresponding author: Dillon J. Amaya, dillon.amaya@noaa.gov, 816-916-8348

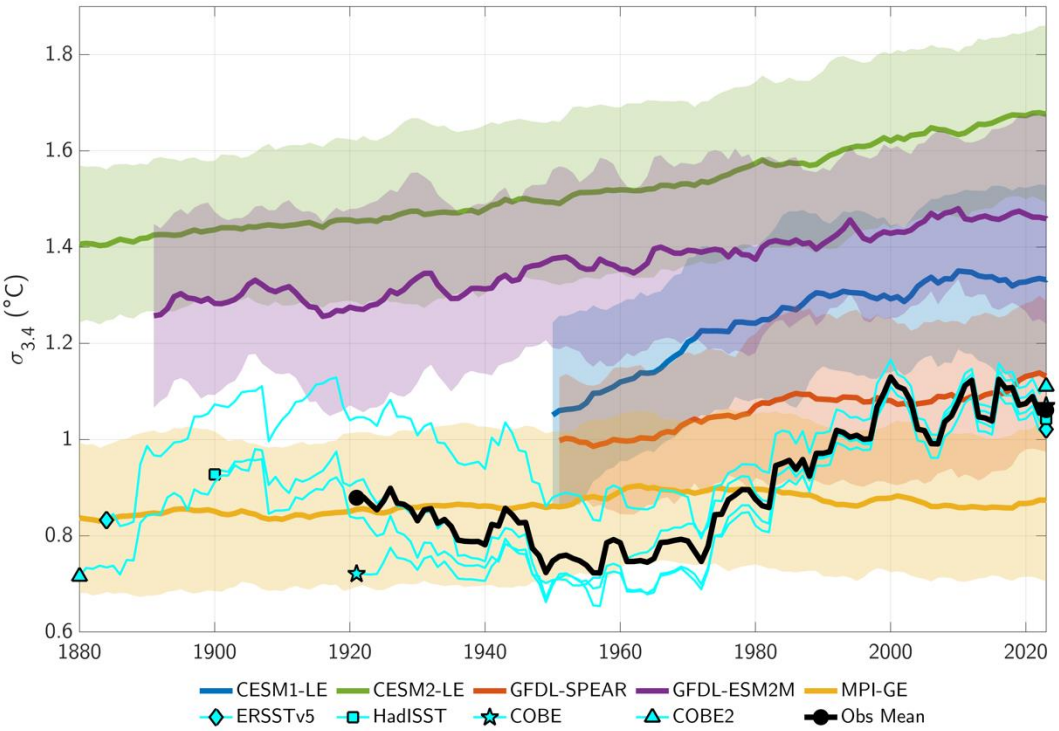

Figure S1 Standard deviation of December-February averaged SSTA in the Nino3.4 region in running 30-year windows from 1851-2023. Years indicate end of the window (e.g., 1960=1931-1960). Colors represent different model large ensembles, with thick curves for ensemble mean values and shading for one standard deviation spread across the ensemble. Cyan curves show the observed values from four different observational products. The black curve is the observational average.

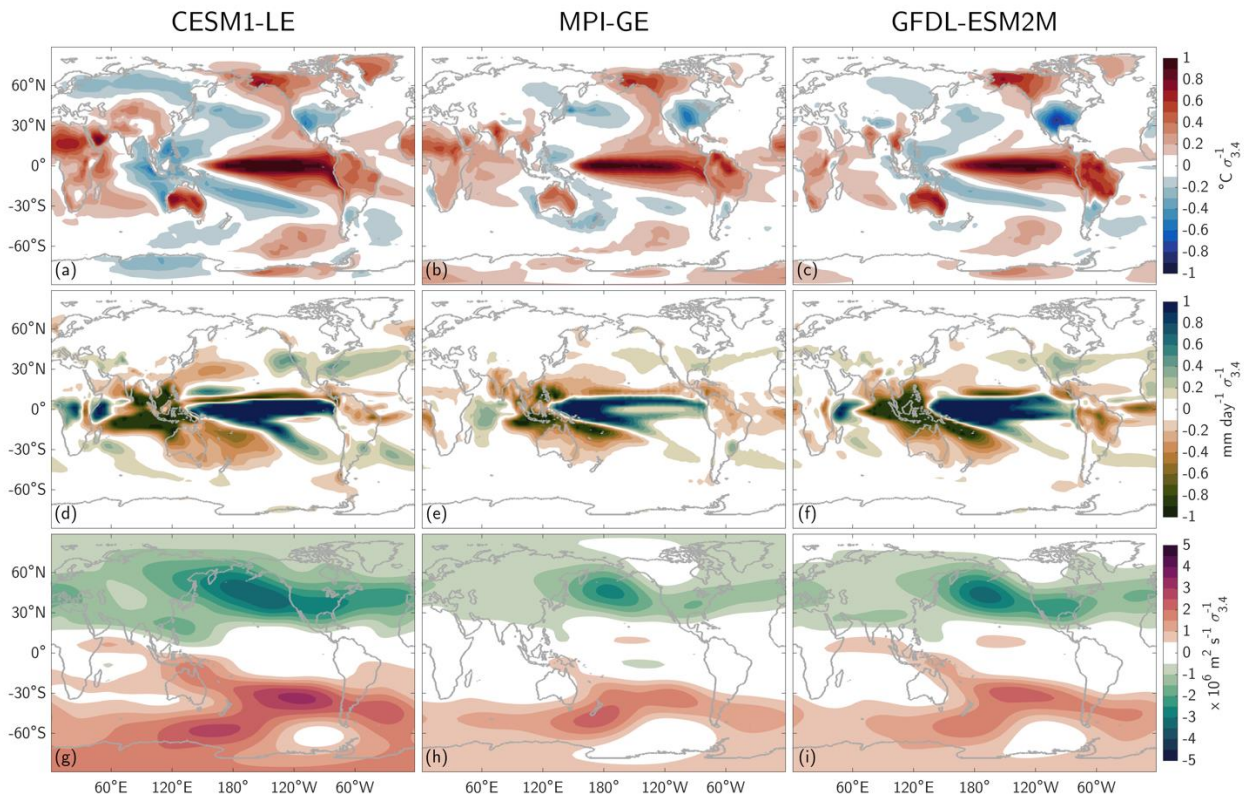

Figure S2 Linear regression of (a)-(c) surface temperature anomalies, (d)-(f) precipitation anomalies, and (g)-(i) 500mb stream function anomalies on the normalized Nino3.4 index in CESM1-LE, MPI-GE, and GFDL-ESM2M, respectively. Regressions are for the period 2071-2100 (results are similar for regressions during the period 1921-1950). Note that pattern correlations reported in the main text are based on the absolute value of these maps.

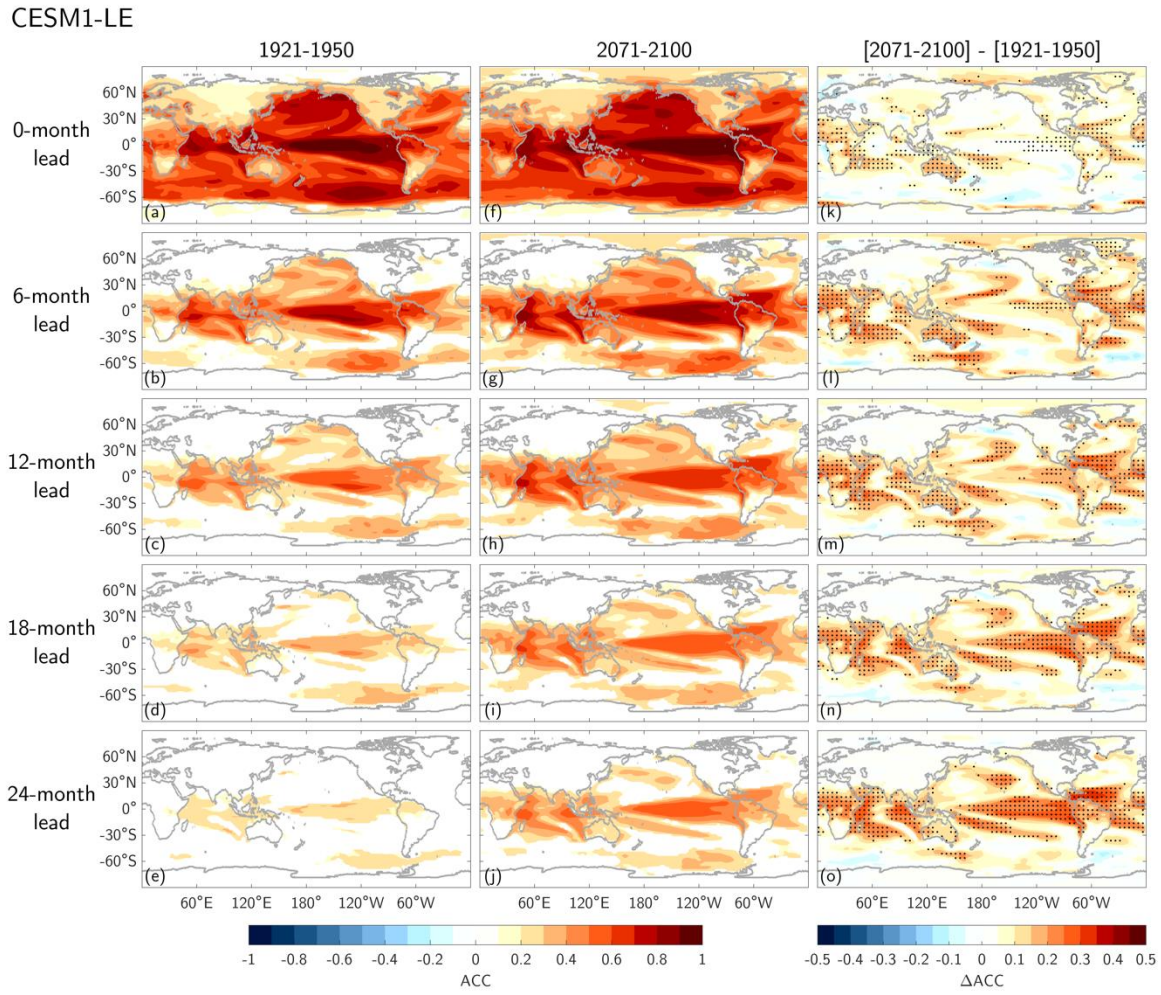

Figure S3 (a)-(e) Ensemble mean potential forecast skill of surface temperature anomalies in CESM1-LE as measured by ACC calculated across all months in the period 1921-1950. (f)-(j) As in (a)-(e), but for the period 2071-2100. (k)-(o) Change in ACC between past and future periods. Skill values in (a)-(j) are only shown when 95% significant. Stipples in (k)-(o) indicate where 90% of the CESM1-LE ensemble agrees on the sign of the change.

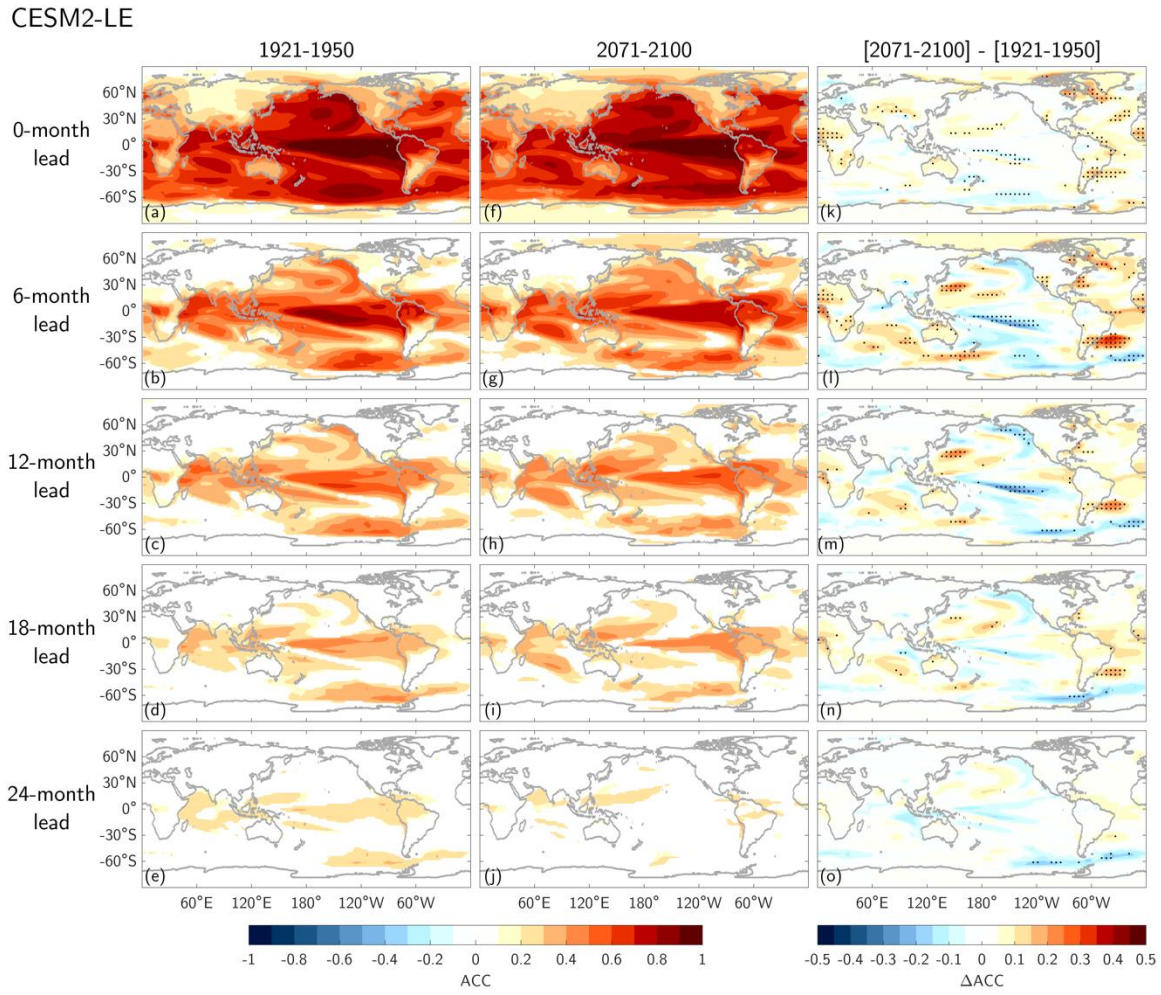

Figure S4 As in Figure S3, but for CESM2-LE.

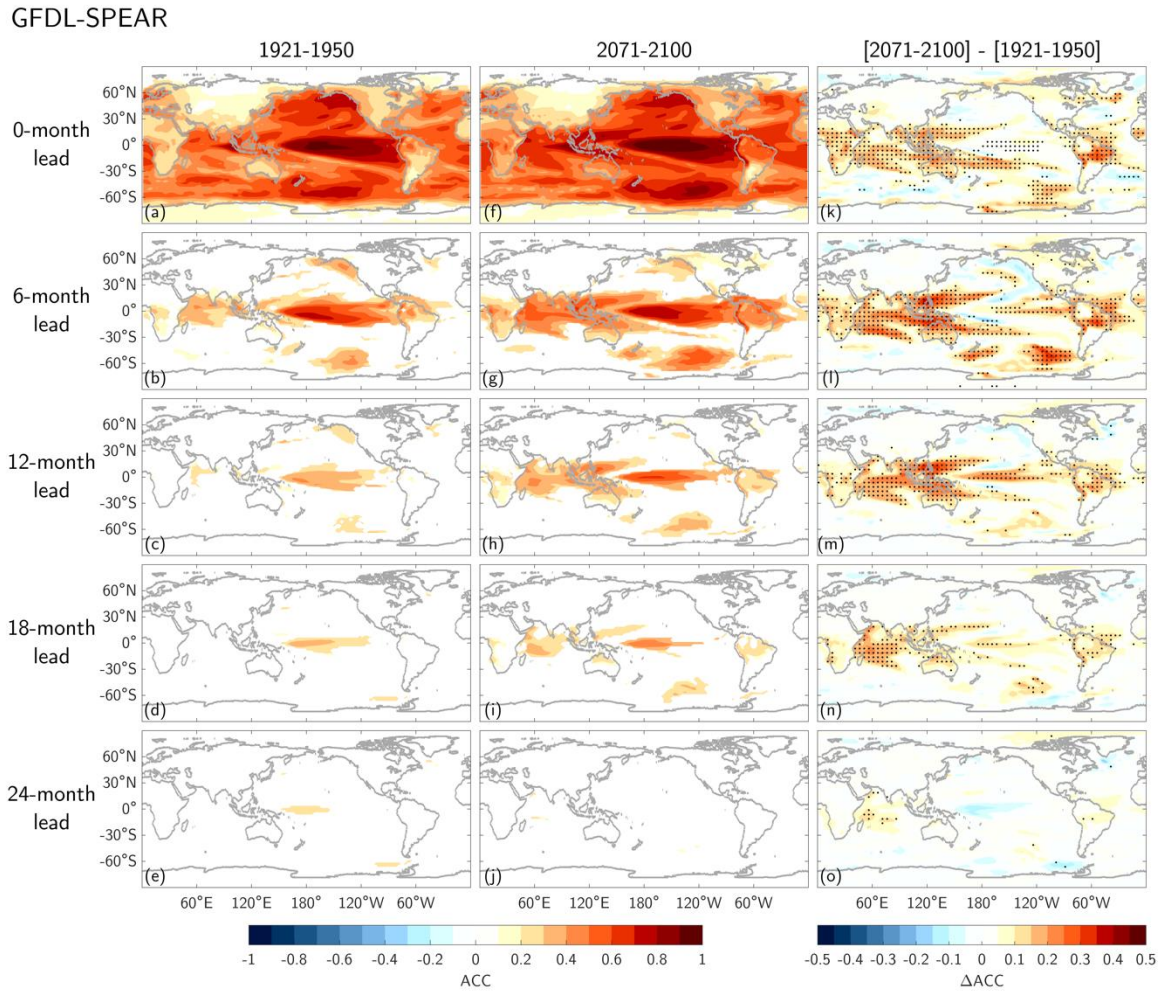

Figure S5 As in Figure S3, but for GFDL-SPEAR.

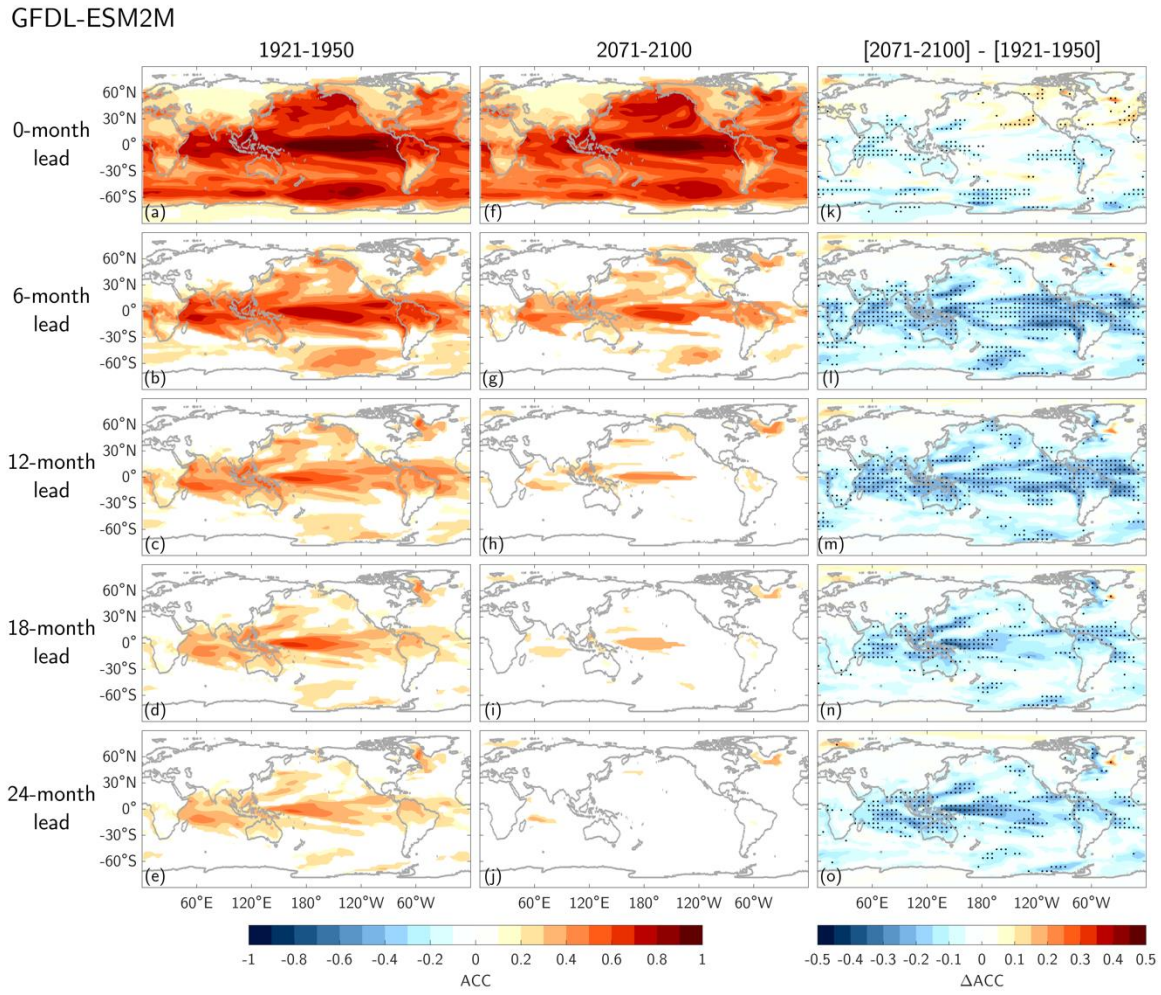

Figure S6 As in Figure S3, but for GFDL-ESM2M.

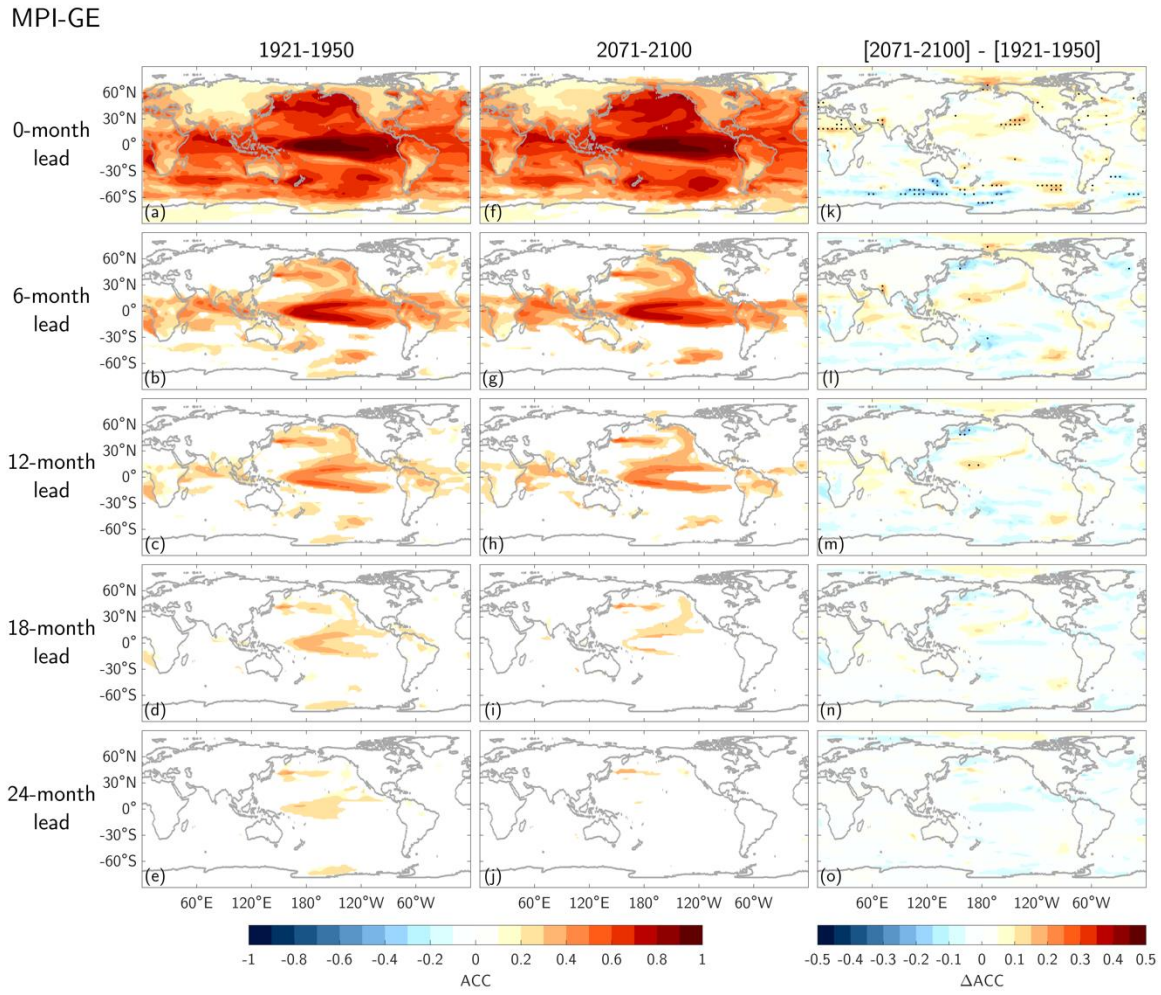

Figure S7 As in Figure S3, but for MPI-GE.

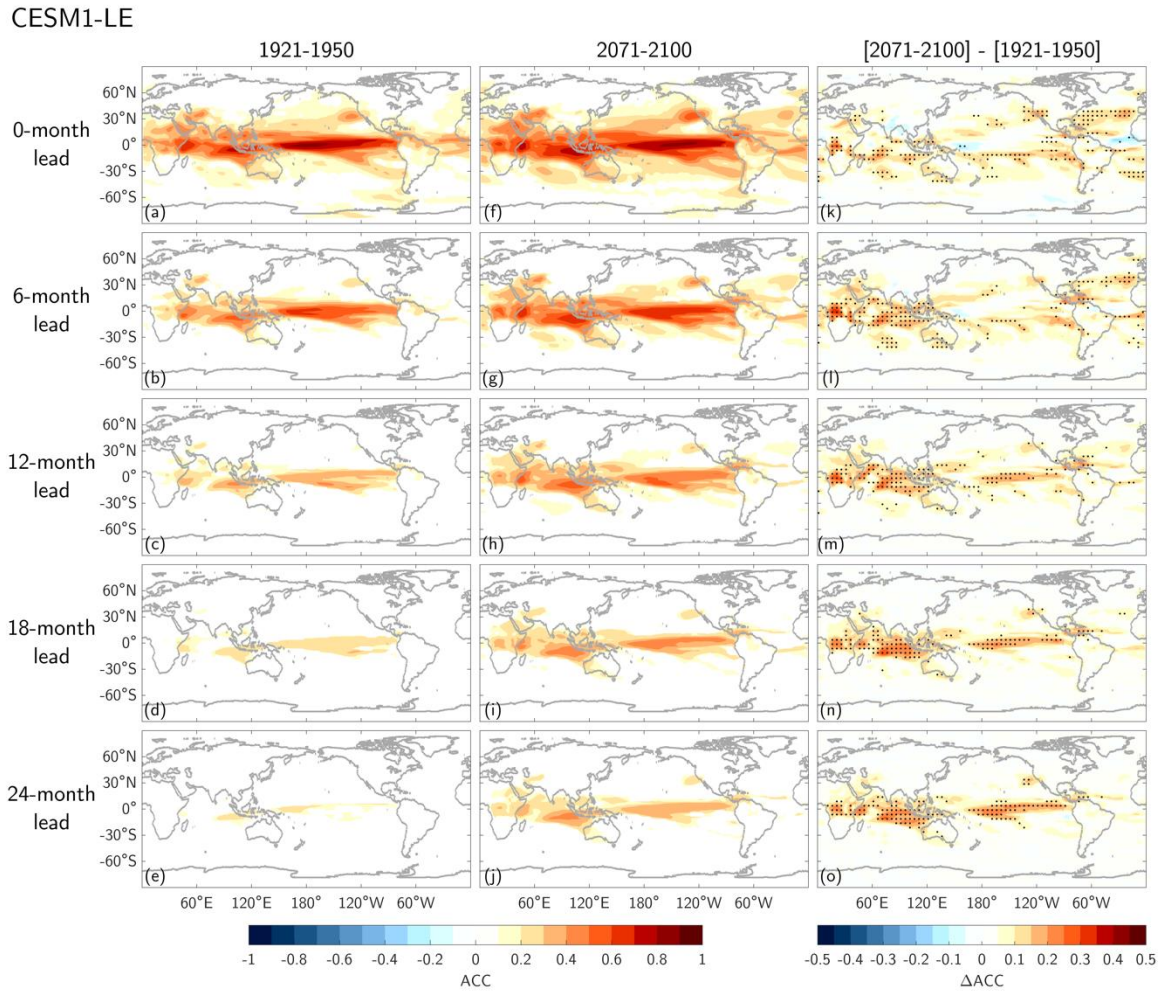

Figure S8 (a)-(e) Ensemble mean potential forecast skill of precipitation anomalies in CESM1-LE as measured by ACC calculated across all months in the period 1921-1950. (f)-(j) As in (a)-(e), but for the period 2071-2100. (k)-(o) Change in ACC between past and future periods. Skill values in (a)-(j) are only shown when 95% significant. Stipples in (k)-(o) indicate where 90% of a the CESM1-LE ensemble agrees on the sign of the change.

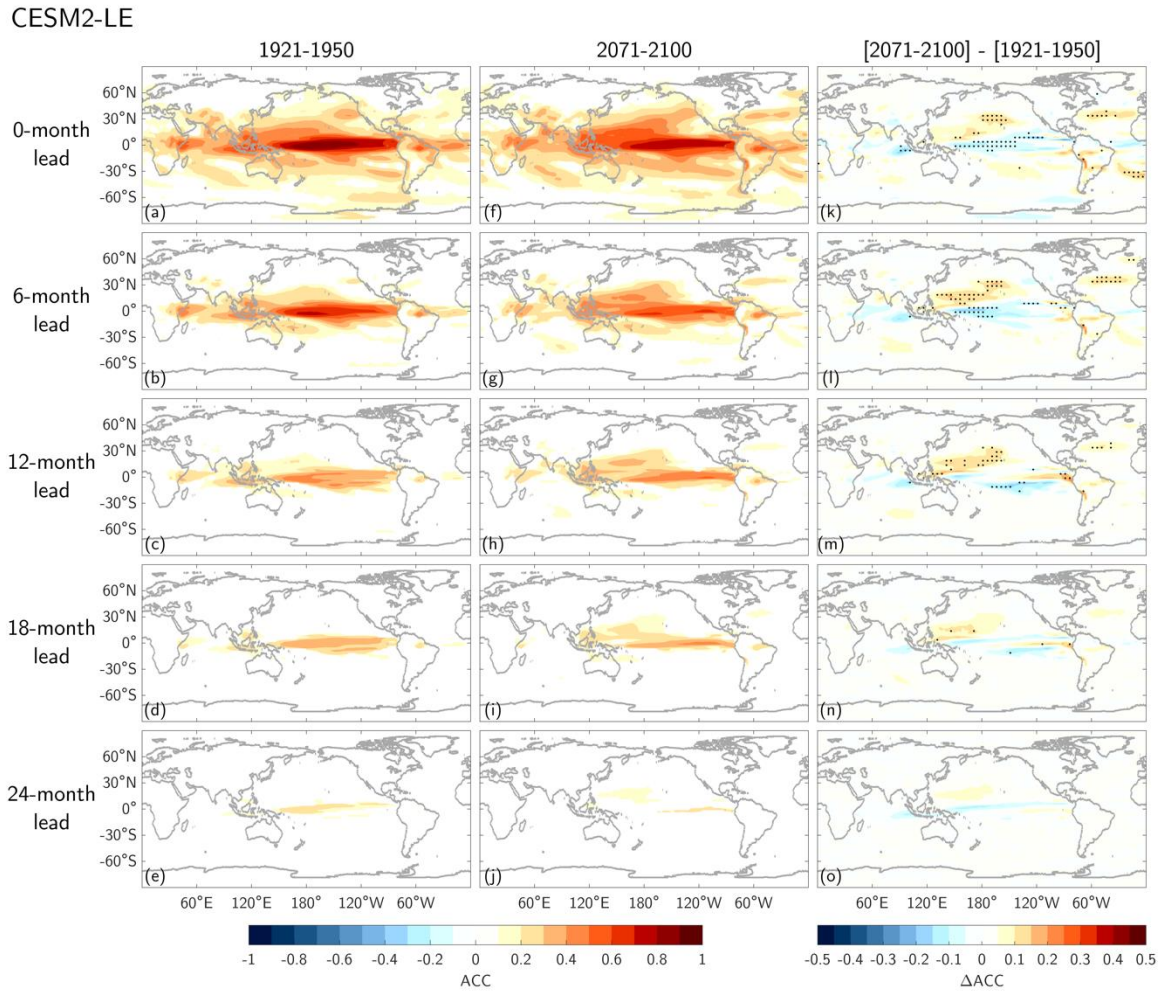

Figure S9 As in Figure S8, but for CESM2-LE.

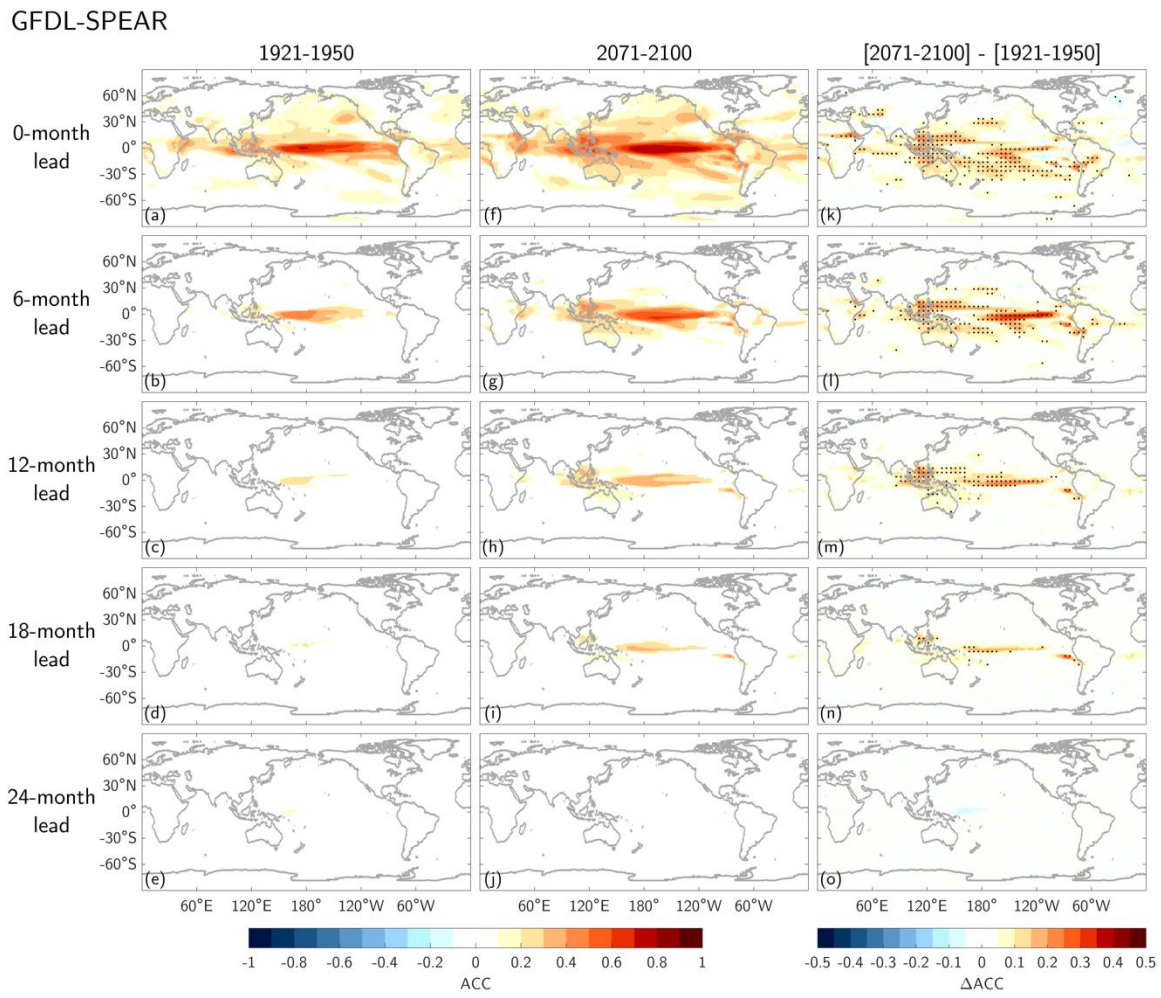

Figure S10 As in Figure S8, but for GFDL-SPEAR.

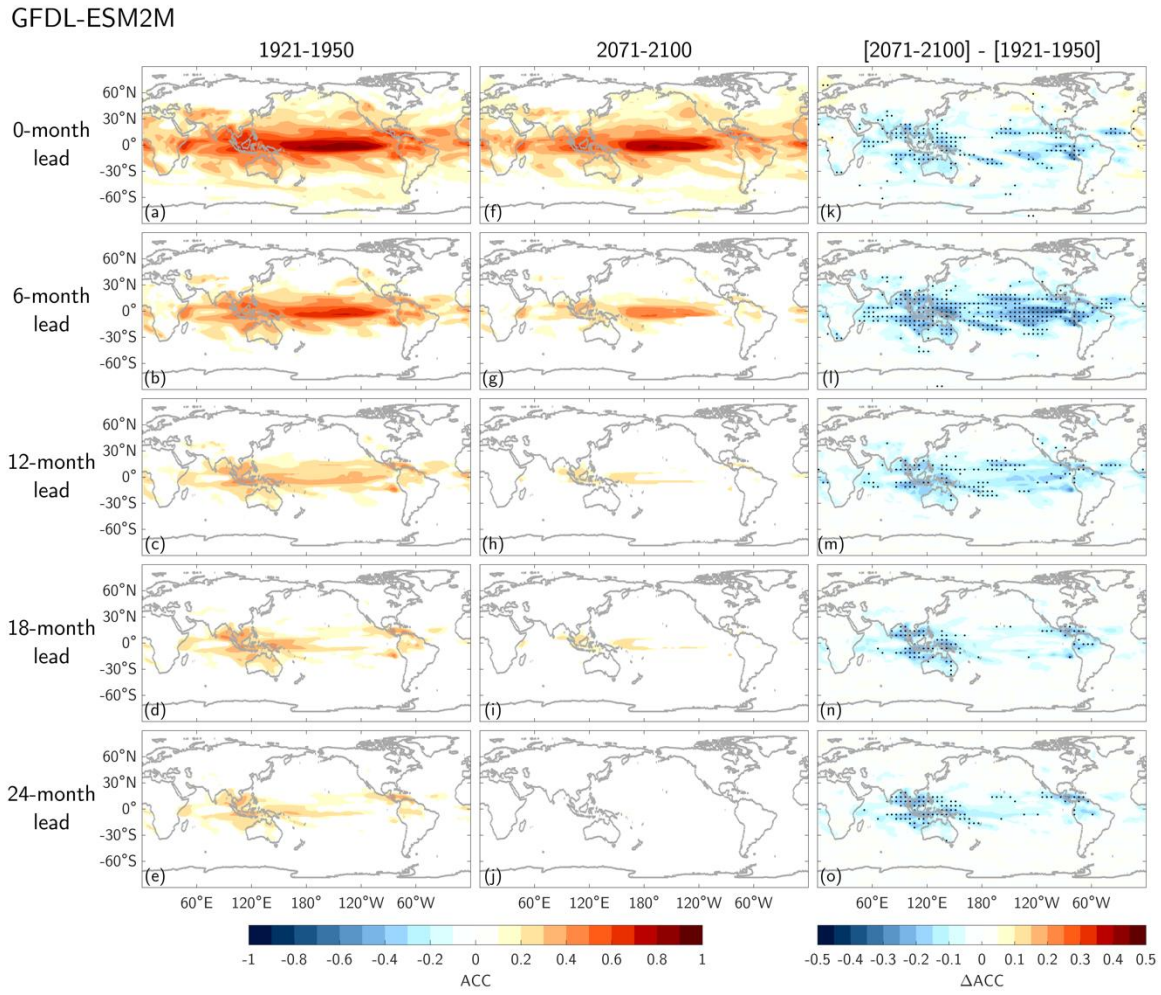

Figure S11 As in Figure S8, but for GFDL-ESM2M.

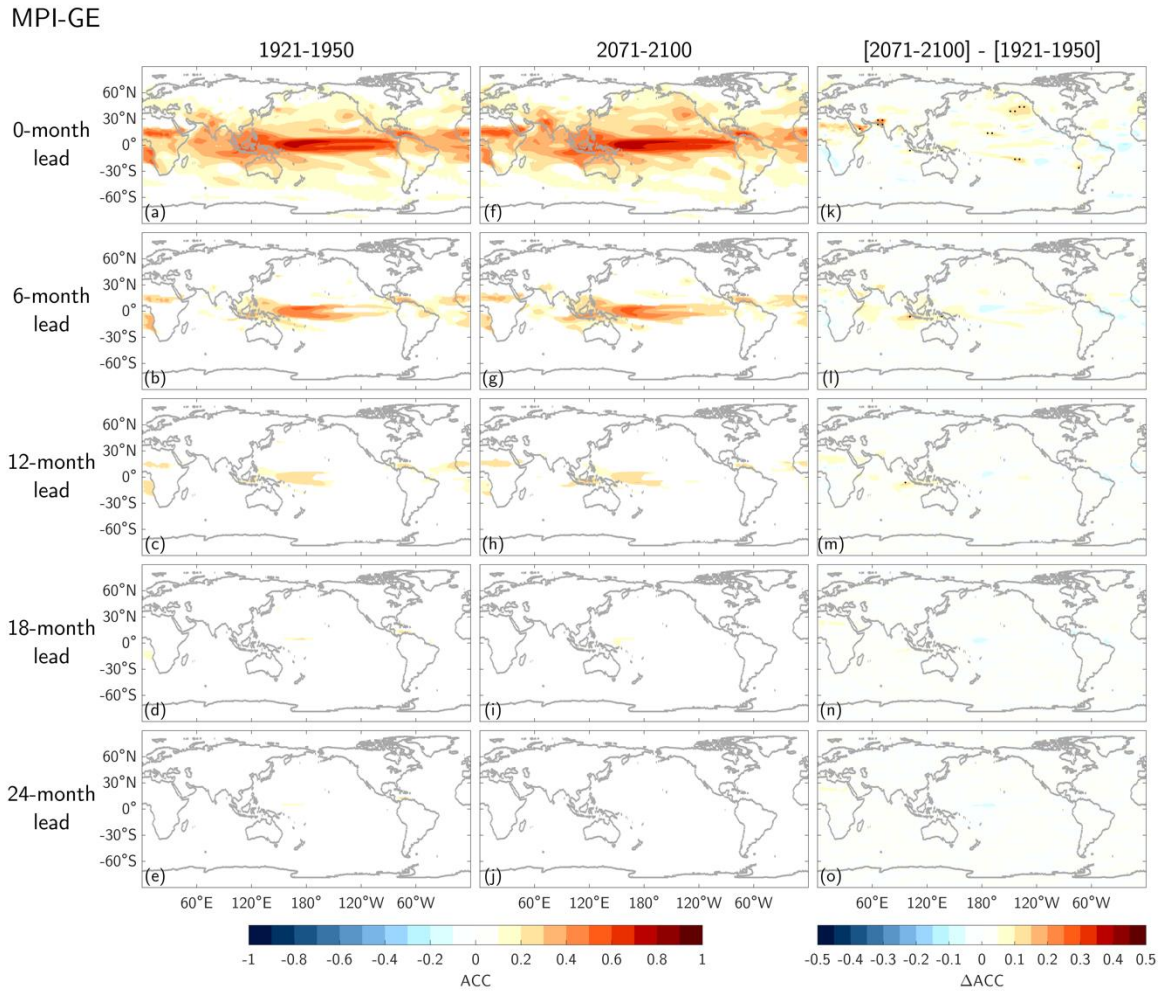

Figure S12 As in Figure S8, but for MPI-GE.

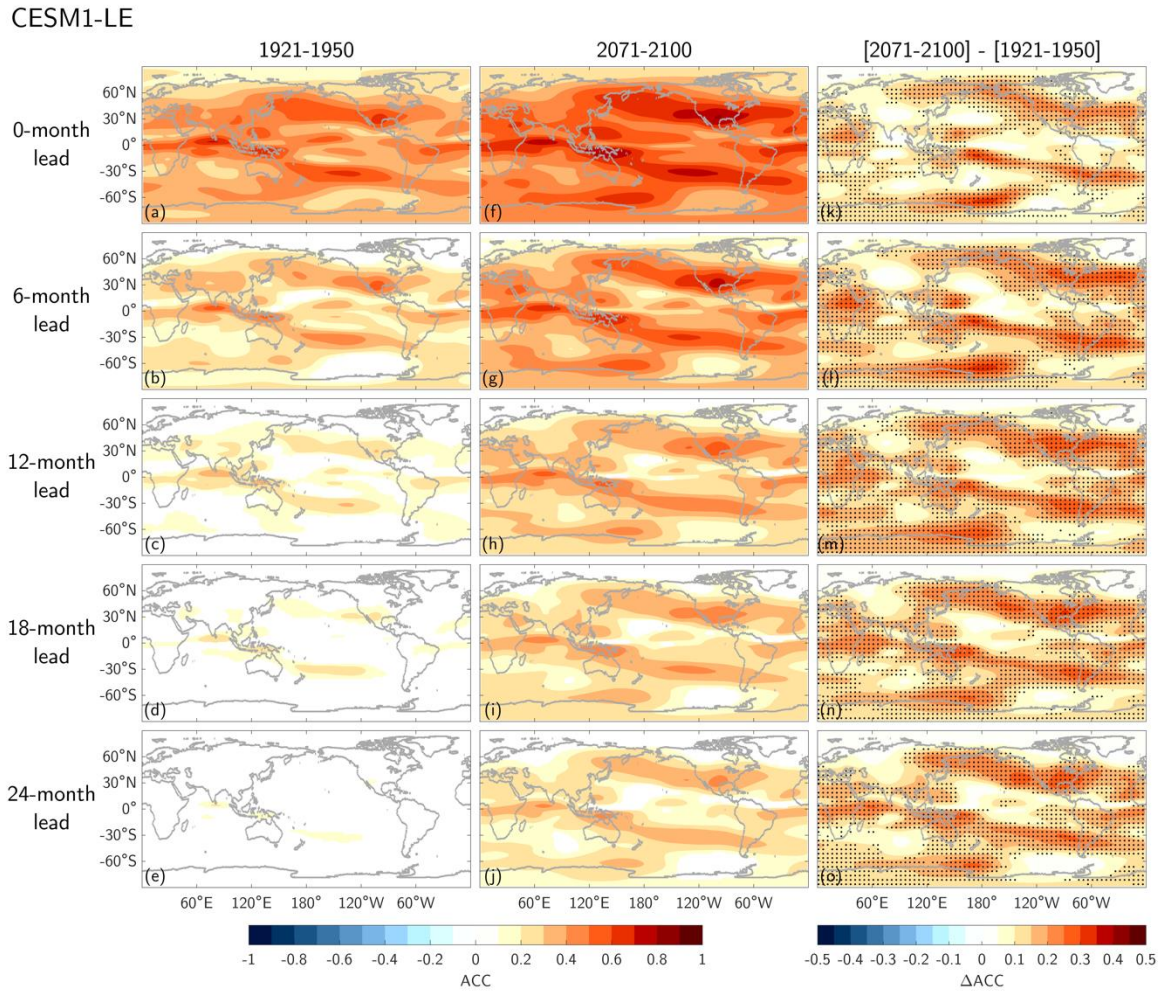

Figure S13 (a)-(e) Ensemble mean potential forecast skill of 500mb stream function (ψ_{500}) anomalies in CESM1-LE as measured by ACC calculated across all months in the period 1921-1950. (f)-(j) As in (a)-(e), but for the period 2071-2100. (k)-(o) Change in ACC between past and future periods. Skill values in (a)-(j) are only shown when 95% significant. Stipples in (k)-(o) indicate where 90% of a the CESM1-LE ensemble agrees on the sign of the change.

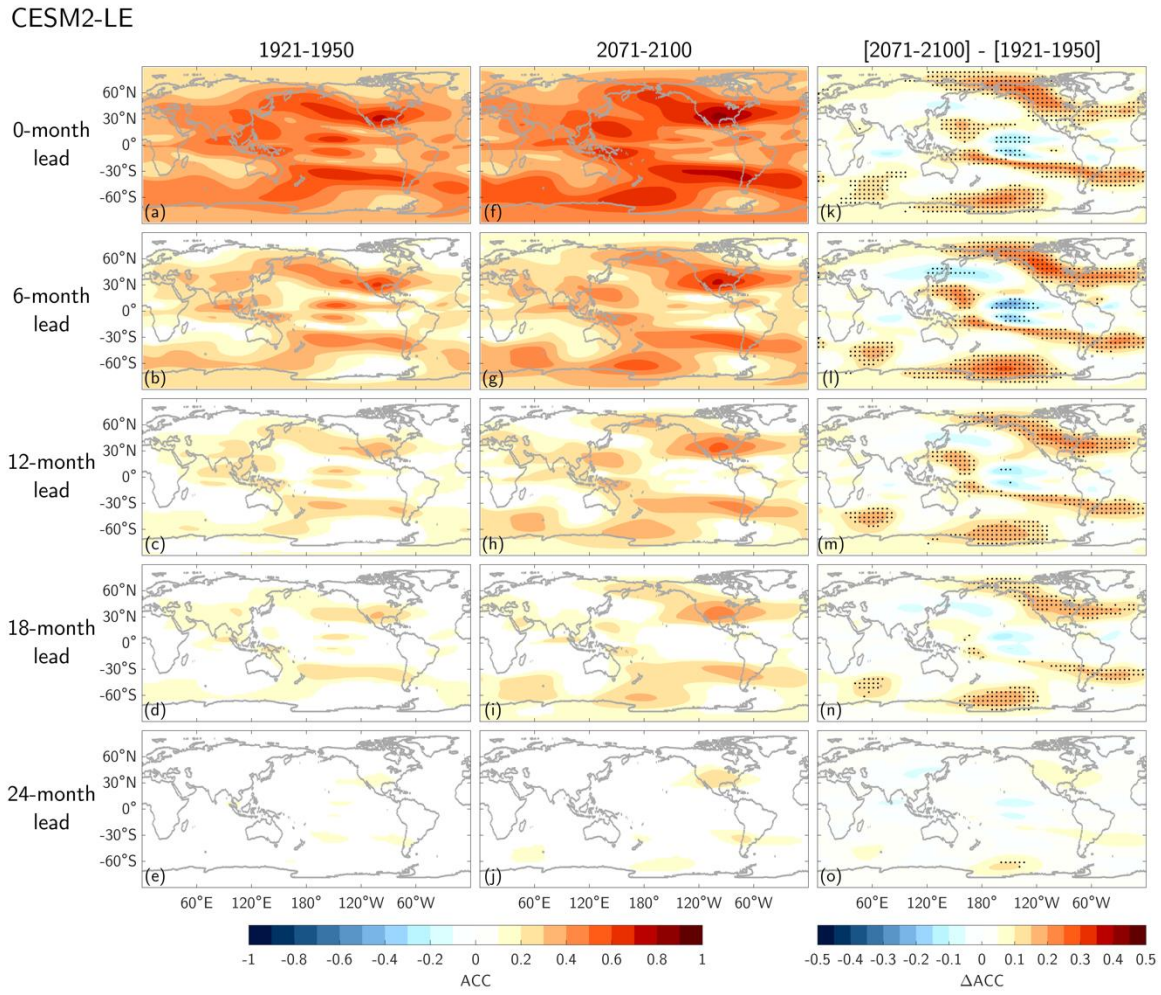

Figure S14 As in Figure S13, but for CESM2-LE.

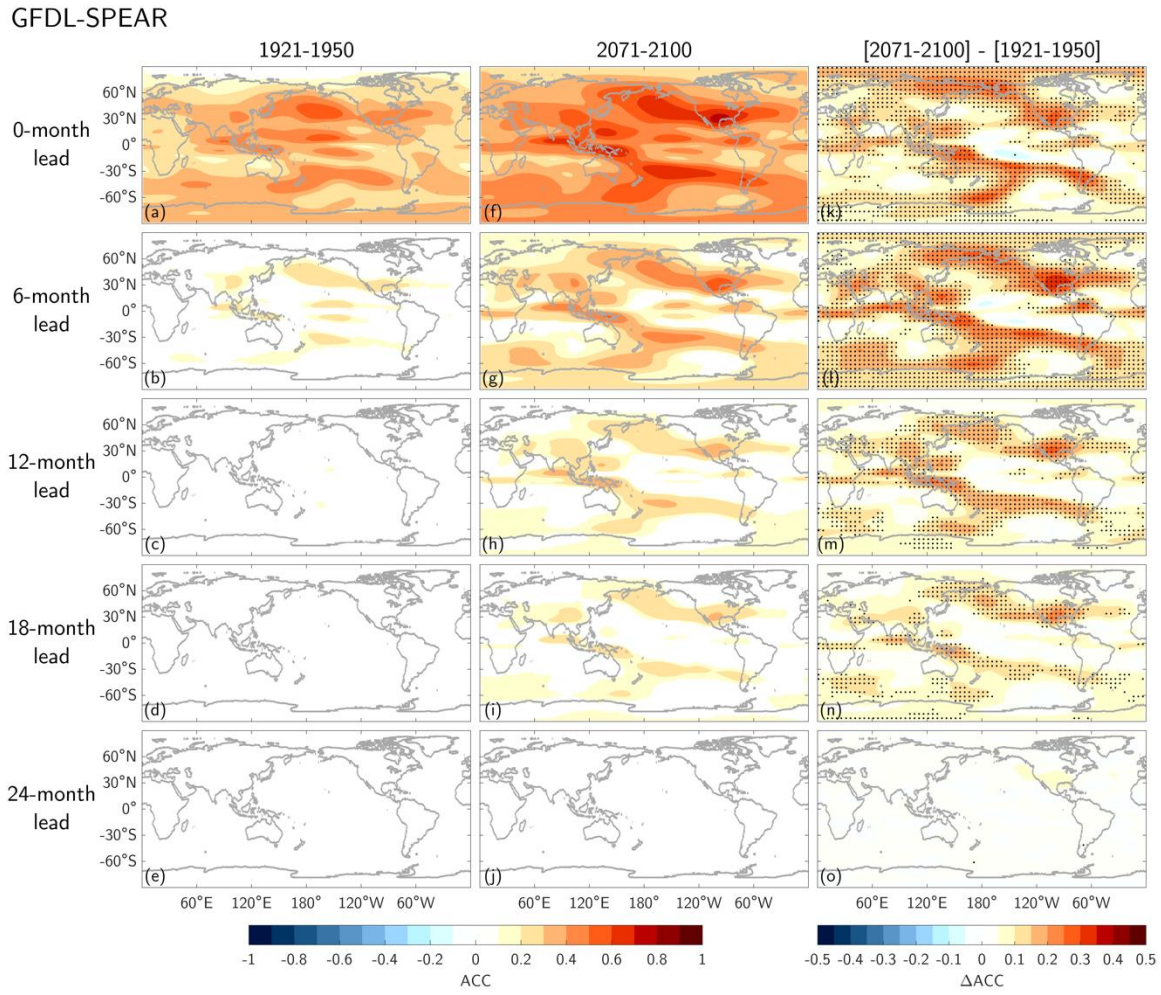

Figure S15 As in Figure S13, but for GFDL-SPEAR.

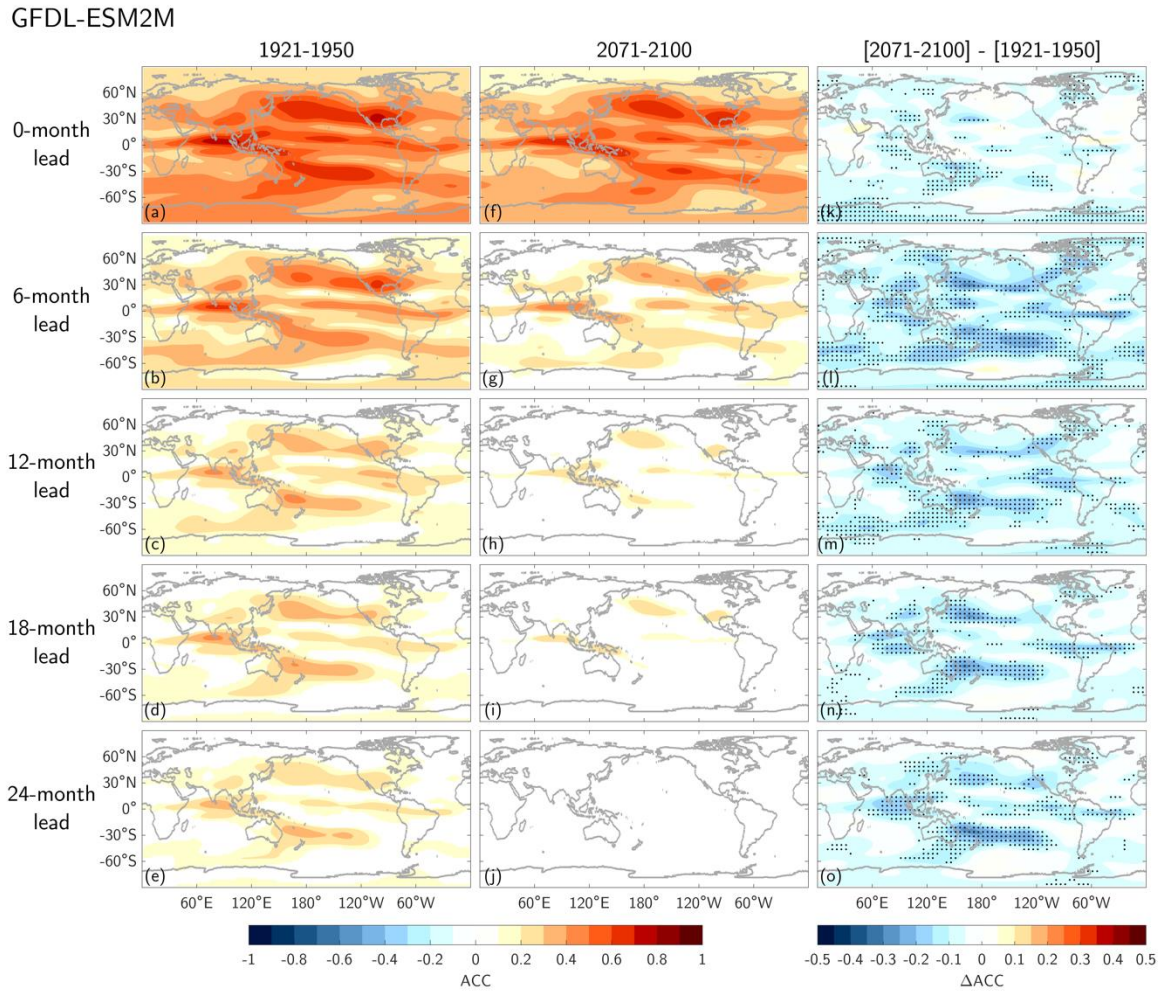

Figure S16 As in Figure S13, but for GFDL-ESM2M.

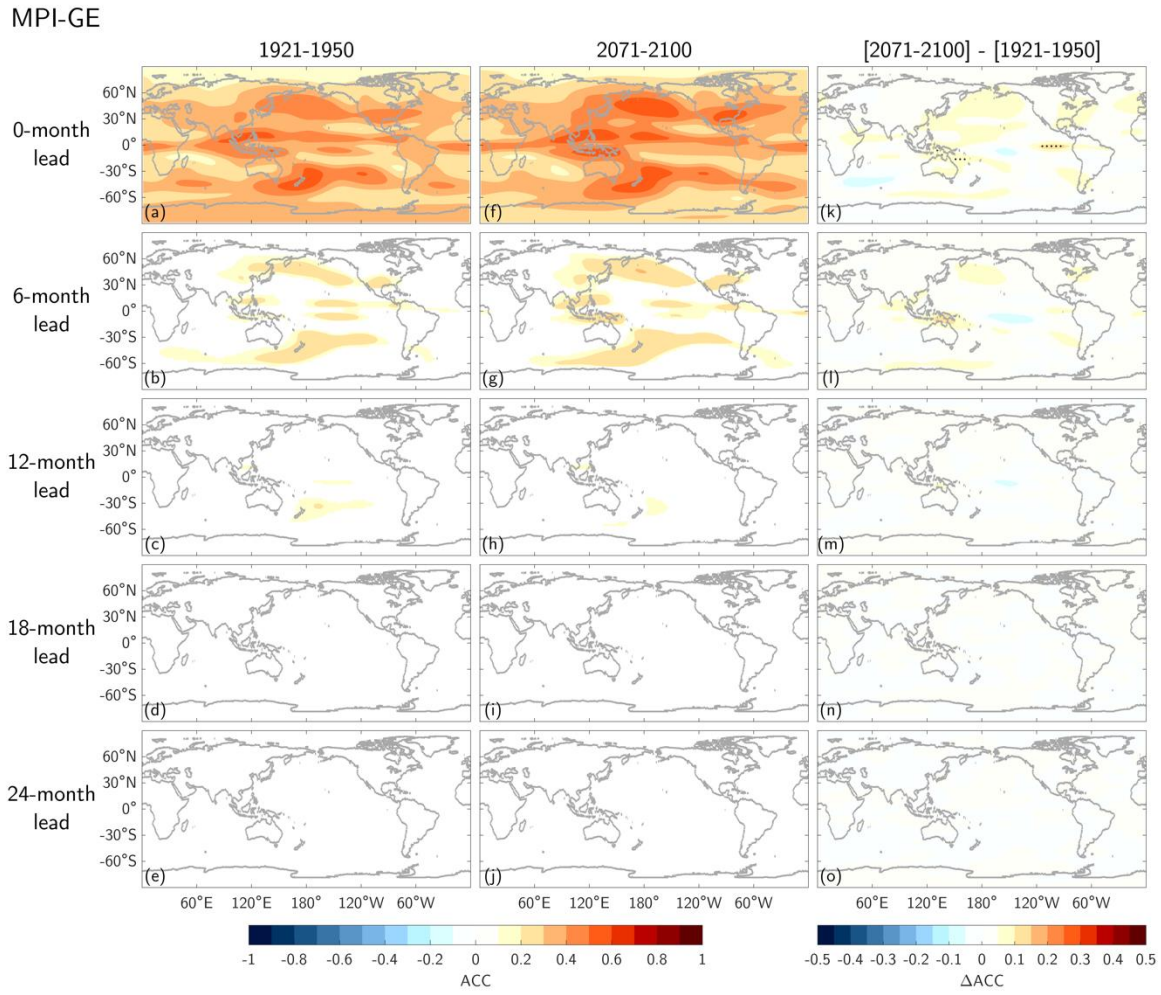

Figure S17 As in Figure S13, but for MPI-GE.

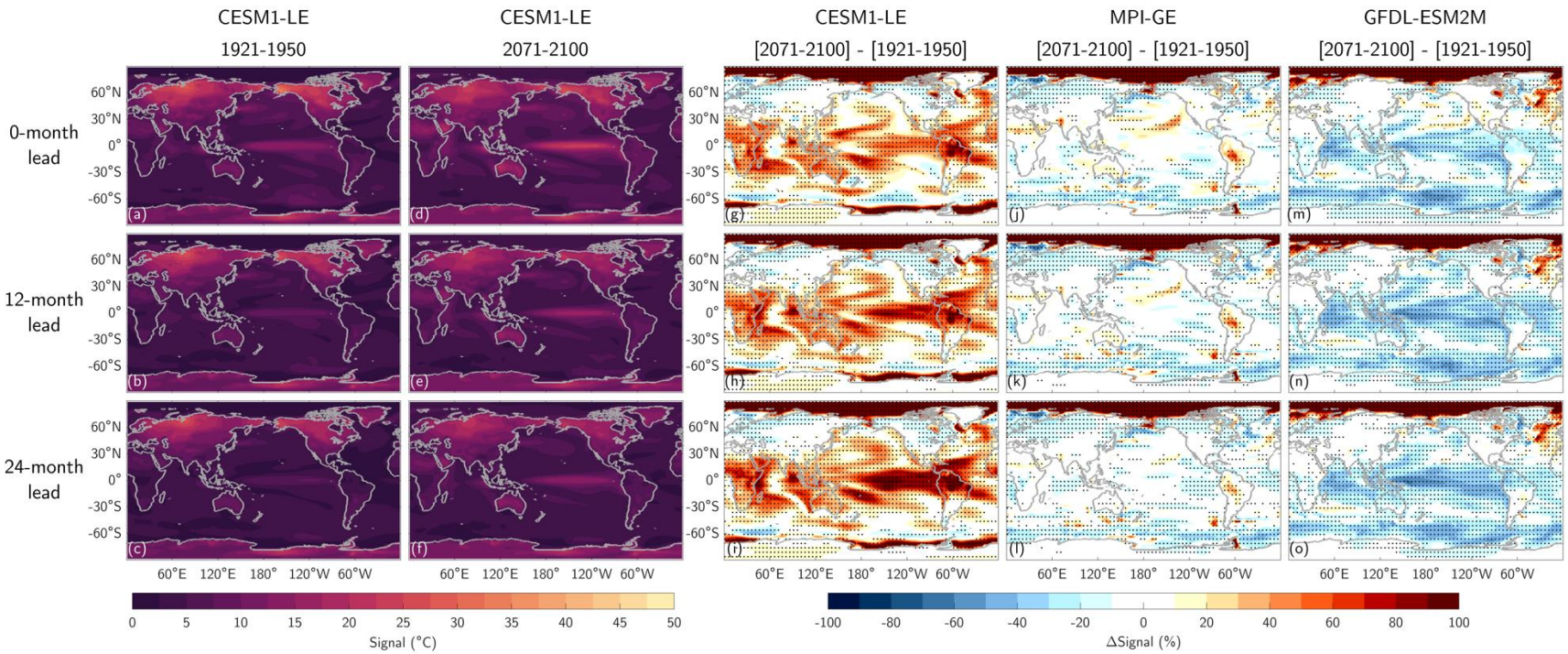

Figure S18 Signal values (˚C) for surface temperature anomaly forecasts (i.e., the numerator of Eq. (1) in main text). (a)-(c) Ensemble mean Signal values of surface temperature forecasts in CESM1-LE calculated across all months in the period 1921-1950. (d)-(f) As in (a)-(c), but for the period 2071-2100. (g)-(o) Percent change in Signal values between past and future periods for (g)-(i) CESM1-LE (j)-(l) MPI-GE (m)-(o) GFDL-ESM2M. Stipples in (g)-(o) indicate where 90% of a respective model's ensemble agrees on the sign of the change.

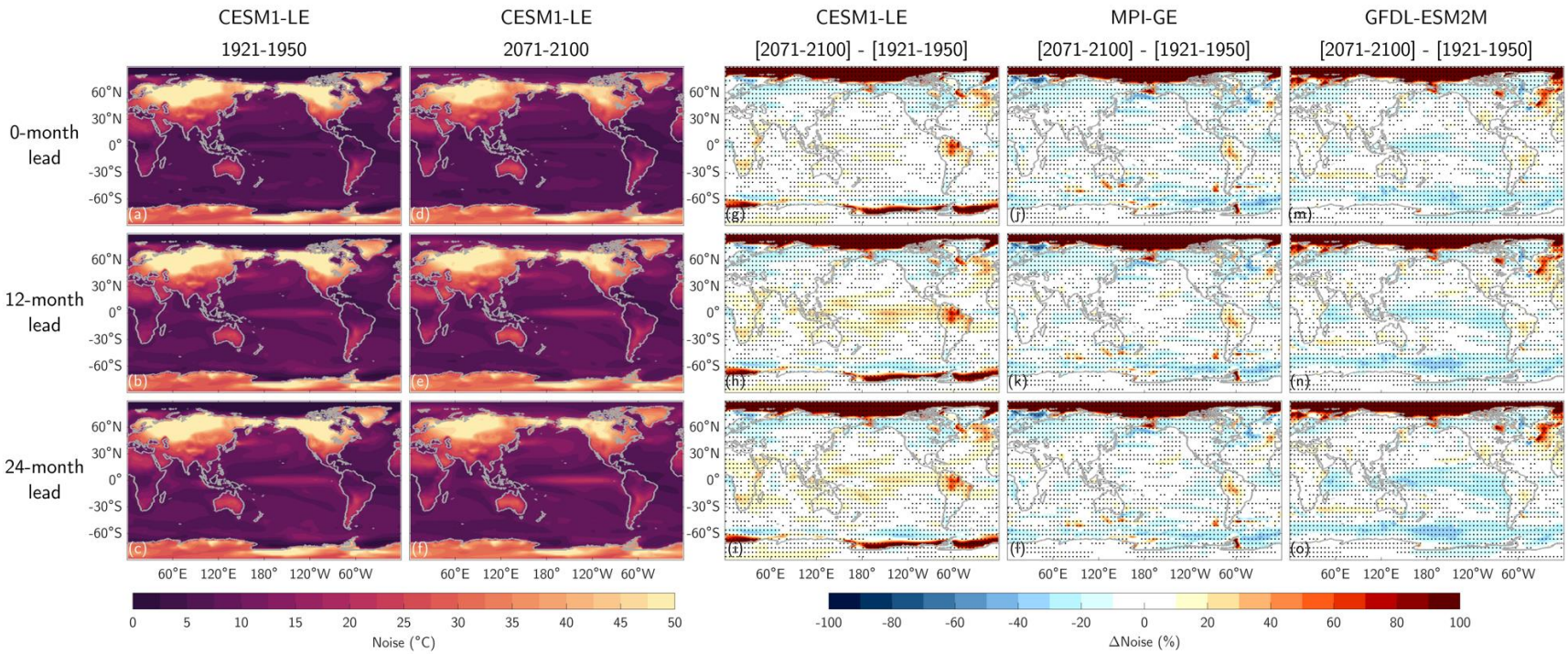

Figure S19 As in Figure S18, but for Noise values (˚C) for surface temperature anomaly forecasts (i.e., the denominator of Eq. (1) in main text).